I.A.U
Karaj branch

Journal of
A p p l ied
C hemical
R esearch
jacr.kiau.ac.ir

Journal of Applied Chemical Research, 16, 4, 45-64 (2022)

Green Fabrication of Albizia Lebbeck Leaves-Capped Silver Nanoparticles for Removal of Butylparaben

Fatemeh Maghami[1], Maryam Abrishamkar[*2], Bijan Mombini Godajdar[1], Mina Hossieni[1]

[1]Department of Chemistry, Omidiyeh Branch, Islamic Azad University, Omidiyeh, Iran

[2]Department of Chemistry, Ahvaz Branch, Islamic Azad University, Ahvaz, Iran

(Received 19 Feb. 2022; Final revised received 11 May 2022)

Abstract

Albizia Lebbeck Leaves-Capped Silver Nanoparticles (ALLC AgNPs) were constructed using a green and sustainable method and used as an effective adsorbent for the removal of butylparaben (BP) dye from an aqueous solution. The possible mechanisms for the fabrication of ALLC AgNPs were also investigated and discussed. The proposed adsorbent was characterized and identified using FT-IR, XRD, and SEM techniques. For investigating the influence of affective factors like BP dye concentration, pH, adsorbent dosage, and sonication time on the removal process and achieving optimum conditions, central composite design (CCD) based response surface methodology (RSM) was applied. To investigate the adsorption mechanism and kinetic of the removal reaction, different isotherm and kinetic models were used. The obtained results proved the applicability of fabricated adsorbent as an ideal material for the treatment of pollutants and especially dye molecules.

Keywords: Butylparaben dye, Adsorption, Albizia Lebbeck Leaves-Capped AgNPs, Fabrication mechanism, Isotherm models, Kinetic models.

**Corresponding author*: *Maryam Abrishamkar, Department of Chemistry, Ahvaz Branch, Islamic Azad University, Ahvaz, Iran. Email: abrishamkarmaryam@gmail.com.*

Introduction

Industrial wastewater as an undesirable by-product [1] may contain hazardous pollutants like organic dyes [2] and drugs that can cause some main diseases like cancer, mutation, and skin problems [3]. Parabens (PBs) as chemical materials have been widely applied in different fields. PBs family is included different materials like methylparaben (MP), ethylparaben (EP), propylparaben (PP), and butylparaben (BP) [4]. Despite the broad applications of PBs, they also have some main side effects like allergic diseases (skin allergic) and skin irritation [5]. Also, they can interfere with the body's hormones, most notably reproductive hormones such as estrogen [6] and testosterone, and produce some main illnesses. In some cases, PBs can produce chronic diseases, cancers [7], and a host of developmental disorders and fertility problems [8].

To date, different wastewater treatment technologies have been successfully used for removing a considerable amount of PBs from wastewater. Among different methods, the adsorption process drew researchers' attention worldwide which is due to its unique properties like simple and easy operation, cost-effectiveness, and most importantly high efficiency [9]. The other exceptional attribute of the adsorption process is its applicability for implementation on large [10] and industrial scales [11].

Among different adsorbents, nano-based materials have been in hotspots [12]. This is due to the exclusive features of these materials in terms of high chemical and physical stability, a large number of reaction sites, a large number of functional groups, high surface area, and high adsorption capacity. Between different nano-based materials, AgNPs have been used in different fields and especially in pollutants treatment as adsorbents. The wide applications of AgNPs can be related to their brilliant properties like localized surface plasmon resonance as well as their antimicrobial and antibacterial features [13].

One of the interesting methods for the synthesis of AgNPs is the application of natural sources like plants [14]. This is considered a green and sustainable method [15]. Green strategies for the synthesis of AgNPs use different organisms, plants being the focus of attention due to their exclusive properties in terms of easy availability, inexpensive nature, non-toxicity, eco-friendliness, as well as suitability for large-scale biosynthesis of AgNPs. The AgNPs generated by plant extracts are more stable and are available in different sizes and shapes as they incorporate unique properties of plant constituents in the assembly of NPs. Till now, several studies have been focused on the synthesis of ALLC AgNPs and their applications in various areas. For instance, Niknam and Marahel [16] synthesized ALLC AgNPs and used them as a sensor for the determination of the megestrol drug. In this work,

$NaBH_4$ was used as a modifier. Despite the application of the work, it has some main disadvantages which can limit its practical applications. For example, the formation mechanism of ALLC AgNPs was not examined and discussed by the authors. Moreover, in this work, the effect of different factors in the determination process was investigated using the one-factor at-a-time (OFAT) method. OFAT can not consider the interactions of factors simultaneously. Also, it can not predict the true optimum levels. In another study, Rafique et al. [17] synthesized AgNPs using Albizia procera leaf extract for dye degradation and antibacterial applications. In this work, the formation mechanism of AgNPs was illustrated. Moreover, the authors investigated the concentrations of leaf extract at room temperature on synthesis as well as on the physical and structural properties of AgNPs.

Domínguez and co-workers [18] prepared AgNPs using an aqueous extract of AL benth seed (ALS) using a sunlight-driven phytochemical synthesis method. Infrared spectroscopy analysis of the ALS extract confirmed the presence of functional groups, characteristics of reducing carbohydrates, and saponins. Besides these works, there are other studies on the synthesis of AgNPs. Although these works are useful, they also have some main drawbacks. For instance, most of these methods need the consumption of a large volume of hazardous and harmful solvents and reagents which makes them expensive and dangerous methods. Also, most of these methods are multi-step and time-consuming. In addition, some of these methods are labor efforts. In this regard, addressing these main limitations seems to be vital. So, to remove these critical drawbacks, in this study, AgNPs were fabricated from Albizia Lebbeck Leaves. Compared to some applied methods, the proposed approach in this work is considered green, simple, easy, and environmentally friendly. These properties are considered the novelty aspects of the present work. Moreover, the applied method in this work is time-saving and most importantly inexpensive. Most importantly, it can be used for the synthesis of AgNPs on large and industrial scales. The other novelty aspects of the present work are an investigation of the formation mechanism of AgNPs from Albizia Lebbeck Leaves and assessing the adsorption mechanism of removal of BP by ALLC AgNPs.

Experimental

Instrumentation

To identify and characterize the fabricated adsorbent as well as to do the removal process, all necessary instruments were used as follows: UV-Vis spectrophotometer model V-530 (Jasco Company, Japan) was utilized to investigate the removal process. Fourier transform infrared

(FT-IR) spectra were registered on a PerkinElmer (FT-IR spectrum BX, Germany) to evaluate the functional groups of the fabricated adsorbent. SEM (Scanning electron microscopy: KYKY-EM 3200, Hitachi Firm, China) under an acceleration voltage of 26kV) was utilized to inquire into the morphology of samples. An ultrasonic bath with a heating system (Tecno-GAZ SPA Ultra Sonic System, Italy) at 60 Hz of frequency and 130W of power was employed for the ultrasound-assisted adsorption procedure. The pH/Ion meter (model-728, Metrohm Firm, Switzerland, Swiss) was used for pH measuring. To ensure the precision of tests, Laboratory glassware was soaked all night in 10% nitric acid solution. An NBE ultra thermostat (VEB Prufgerate - WerkMedingen, Germany) was applied to adjust the temperature [19].

Reagents and materials

The possibility of purchasing all the chemicals (silver nitrate ($AgNO_3$), sodium hydroxide, hydrochloric acid) from Merck Company was provided. Also, BP dye and methanol were provided by Sigma Aldrich.

Fabrication of ALLC AgNPs and their possible formation mechanism

The wide utilization of AgNPs in various fields like medicine, pollutants treatment, and producing laundry products (soaps and detergents) has made them popular. Therefore, this broad applicability and most importantly unique properties of AgNPs have cheered us to synthesize and use them for BP removal from aqueous solutions. The preparation of ALLC AgNPs was conducted based on the literature methods. For this purpose, 90.0 mL of $AgNO_3$ (0.1 mM) solution and 10.0 mL of Albizia Lebbeck Leaves (0.1 mM) solution were mixed in a reaction flask and stirred strenuously at 25 °C (Figure 1). The role of $AgNO_3$ was as a reducing and modifying agent. The mixture was kept and then its color was changed from dark to bright yellow which confirmed the fabrication of target ALLC AgNPs. The stability of the ALLC AgNPs solution for several weeks was of great significance.

The formation mechanism of AgNPs is based on the phytosynthesis method. This method is considered an *In vivo* green synthesis method in which different sources like plants, their extract, and fruit juices are used for the construction of metal NPs [20]. In an *In vivo* synthesis method, cations of metallic salts produce hydroxyl complexes after saturation [21]. One of the main mechanisms for the preparation of metal NPs is redox reactions in which the compound in extracted plants like polyphenols and proteins act as ligands (electron donors) and interact with metal ions (Ag^{+}, Au^{3+}, Cu^{2+}, etc.) as electron acceptor and synthesis metal

nanoparticles. The composition of the plant extract is one of the main points in the synthesis of metal NPs. For instance, there are many phytochemicals like amides, aldehydes, terpenoids, flavonoids, ketones, carboxylic acids, and sugars that are responsible for the bioreduction of the precursor salts. The other main compositions of ALLC are carbohydrates and also saponin. Saponin can act as a reducing agent and reduce metal ions and produce metal NPs. Moreover, carbohydrates like monosaccharides galactose, glucose, and fructose are all considered reducing sugars [22]. The aldehyde functional group in their structures allows them to act as a reducing agent and produce metal NPs [23].

The proposed ALLC AgNPs were fabricated at room temperature in this work. This fact can be one of the excellent advantages of the presented work. Using room temperature makes us able to produce a wide range of NPs. Most importantly, the proposed method in the current study did not need to use a heating system and also other expensive and labor efforts equipment. It is worth mentioning that the room temperature synthesis method is considered s a green method that has attracted a lot of attention in recent years.

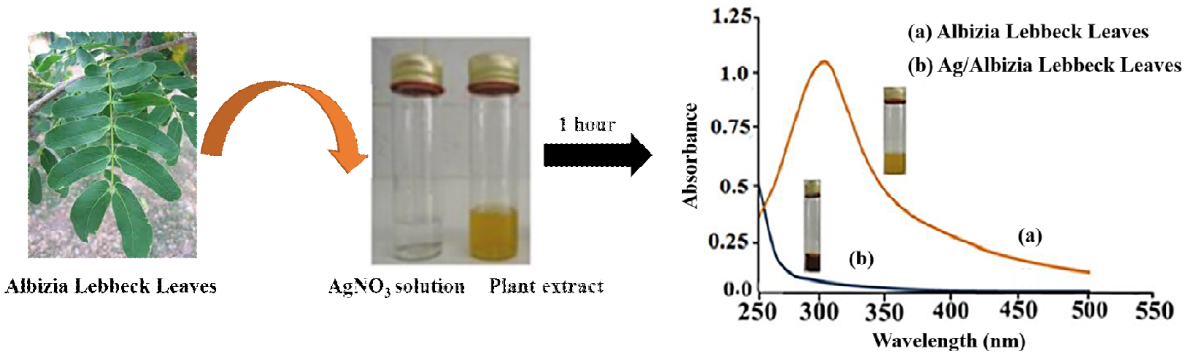

Figure 1. The synthesis procedure of ALLC AgNPs.

Adsorption procedure

The adsorption procedure and the calculations related to removal percentage and maximum adsorption capacity were performed according to our reported articles [24]. The adsorption procedure was conducted according to optimum values from CCD as follows: 50 mL of BP dye solution (12 mg L^{-1}), pH of 7.0, the adsorbent dosage of 0.035 g, and sonication time of 4.0 min.

CCD-based RSM for investigation and optimization of effective parameters

In this work, to evaluate the effects of different parameters and achieve their optimum values, CCD was used. Compared to traditional optimization approaches, CCD is considered a

powerful method [25]. It can reduce the number of experiments and subsequently decrement the cost [26]. Most importantly, CCD can consider the effects of different factors on the removal process concurrently and predict true optimum levels. Effective factors like initial BP concentration (X_1), pH (X_2), adsorbent mass (X_3), and contact time (X_4) were studied at five levels Table 1. In the following, to examine the accuracy of the used model, an analysis of variance (ANOVA) was conducted (Table 2). ANOVA uses a series of statistical analyses like p-value test, F-test, lack-of test, and R^2 for assessing the used model. The other interesting property of CCD is that it can predict an equation that can show the relationship between response and factors. The optimization values can be achieved under the desirability function (DF). DF is a function that has the ability to conversion the response of each factor into a desirability score [27]. DF can get values in the range of 0.0 to 1.0. The values close to 0.0 represent a completely undesirable response while the values close to 1.0 are interesting and show a fully desired response.

Table 1. Factors and the level of each factor.

Factors	**levels**			**Star point α=2.0**	
	Low(-1)	Central(0)	High(+1)	-α	+α
(X_1) BP concentration (mg L^{-1})	20	30	40	10	50
(X_2) pH	5.0	6.0	7.0	4.0	8.0
(X_3) Adsorbent mass (g)	0.015	0.025	0.035	0.005	0.045
(X_4) Contact time (min)	3.0	4.0	5.0	2.0	6.0

Table 2. The Central Composite Design for removal of BP by ALLC AgNPs.

Run	**X_1**	**X_2**	**X_3**	**X_4**	**R% BP**
1	20	6.0	0.025	4.0	92.63
2	30	7.0	0.015	3.0	55
3	10	7.0	0.025	5.0	95
4	20	6.0	0.025	4.0	92.5
5	30	5.0	0.015	3.0	73
6	10	7.0	0.035	4.0	99.18
7	20	4.0	0.025	4.0	96
8	20	6.0	0.025	6.0	93
9	30	5.0	0.035	3.0	80
10	30	5.0	0.015	5.0	90
11	20	6.0	0.025	4.0	93.2
12	30	7.0	0.015	5.0	70.76
13	30	7.0	0.035	5.0	80.4
14	10	7.0	0.015	3.0	95
15	20	6.0	0.025	4.0	93
16	30	5.0	0.035	5.0	93.5

17	20	6.0	0.025	4.0	93.12
18	10	7.0	0.025	3.0	93.66
19	10	7.0	0.035	5.0	97.66
20	10	5.0	0.035	5.0	95
21	10	7.0	0.030	4.0	100
22	50	6.0	0.025	4.0	58.73
23	30	7.0	0.035	3.0	65
24	20	6.0	0.025	4.0	93.62
25	10	7.0	0.045	4.0	93.52
26	20	6.0	0.005	4.0	90
27	20	6.0	0.025	2.0	75
28	20	8.0	0.025	4.0	82
29	40	7.0	0.035	4.0	95
30	20	7.0	0.030	4.0	100

Artificial neural networks (ANN)

For the simulation of the applied removal process, ANN was used. The principles of ANN are presented in the literature [28].

Result and discussion

Identification and evaluation of the ALLC AgNPs

As can be seen from Figure 2., the XRD pattern of the ALLC AgNPs displayed signals at 38.5 (122), 45.0 (111), 52.2 (200), 54.4 (231), and 72.7 (220) which were related to carbon atoms [29]. After functionalizing with activated carbon, as it was apparent to a great extent, the nature of the prepared particles from Albizia Lebbeck Leaves was crystalline. However, a small amount of material was in the amorphous state which was confirmed by the high intensity of the signal at 45.0 (111). The observed XRD pattern proved the formation of activated carbon from ALLC AgNPs. In Figure 3, the FT-IR spectrum of activated carbon prepared from ALLC AgNPs was shown. Additionally, the observed absorption signal at 3451 cm^{-1} point to O-H groups' presence because of the alcoholic or phenolic functional groups. Also, the presence of C-H groups was well proven by the signal observed at 3101 cm^{-1}. Correspondingly, the C=O active group's presence was confirmed by the signal observed at 2158 cm^{-1}. The signal at 776.8 cm^{-1} was relevant to the Ag-O group of the ALLC AgNPs. Scrutinizing these functional groups was of great consequence since complexation, or electrostatic attraction between the metal ions and varied surface oxygen-containing functional groups carried by the activated carbons leads to the elimination of heavy metals.

In Figure 4, the morphological properties of the investigated samples were demonstrated by SEM. Based on Figure 4, it was evident that ALLC AgNPs were even, homogeneous,

shipshape, and almost uniform in size distribution. However, they changed to be uneven, larger, and accumulated after surface modification with activated carbon prepared from ALLC AgNPs.

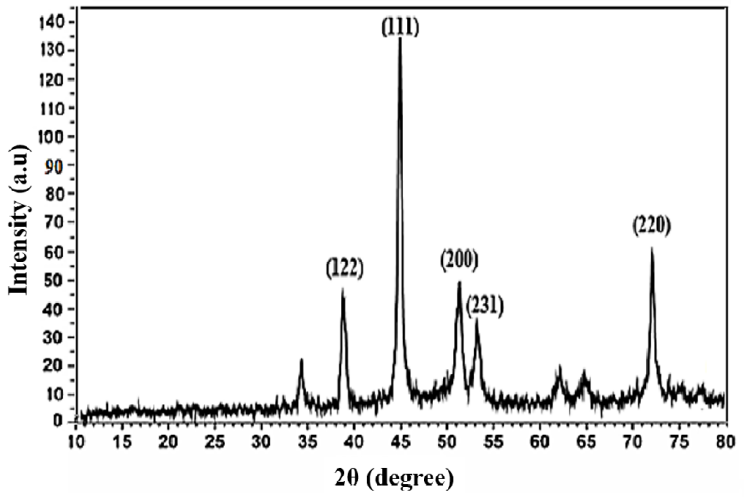

Figure 2. The XRD image of the prepared ALLC Ag NPs.

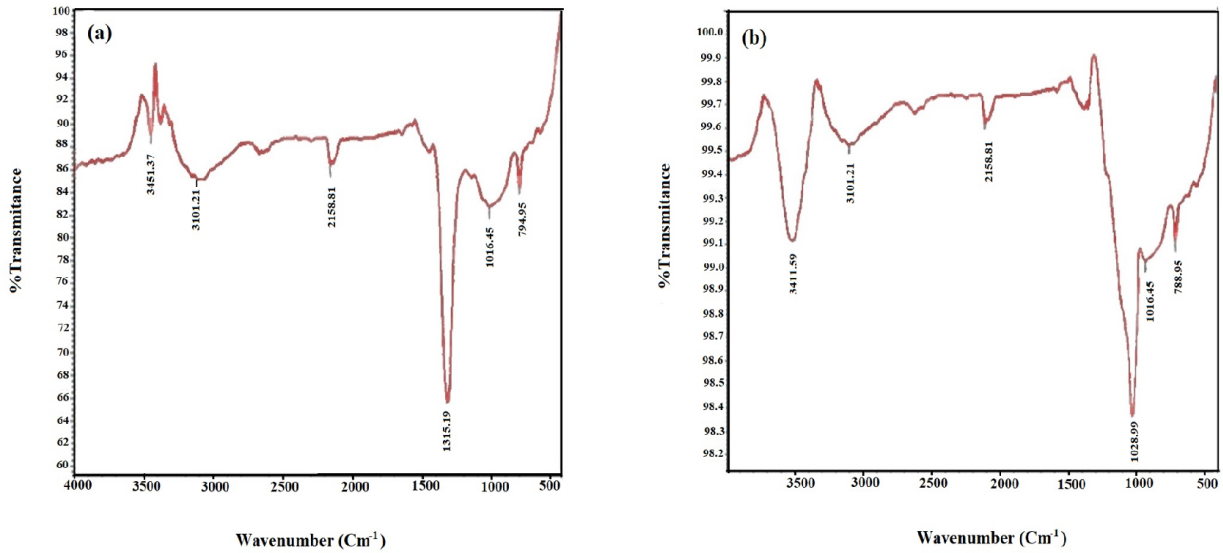

Figure 3. FTIR spectra of the prepared ALL (a), FTIR spectra of the prepared ALLC AgNPs (b).

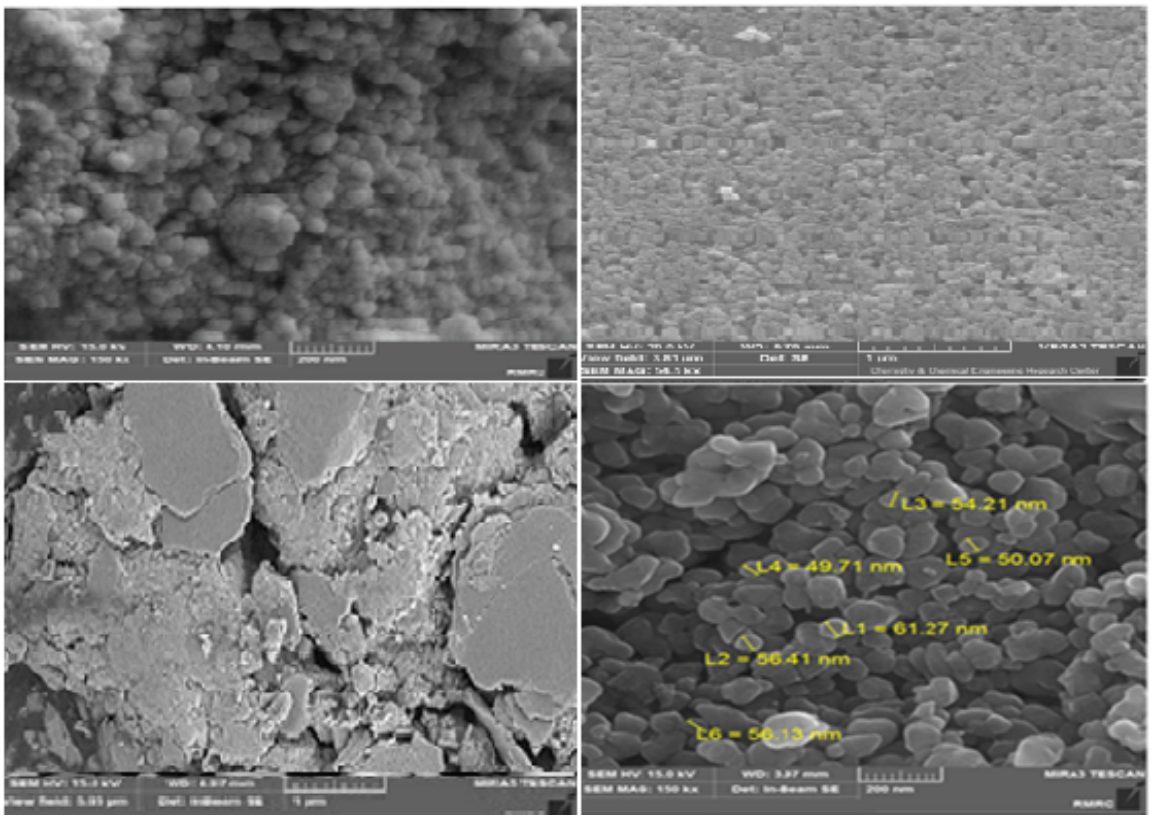

Figure 4. The SEM images of the ALLC AgNPs.

ANOVA analysis

To investigate the accuracy of the used model, ANOVA was used (Table 3). The performance of the model was assessed at a certain confidence level (α = 0.05). In addition, the adaptability of the model was assessed using the p and F test in which the parameters with a p-value less than 0.05 and higher F values had a significant contribution to the removal process. The lack-of-fit value higher than 0.05 (0.080484) approved the precision and dependability of the recommended model [30]. Equation 1 represented the effect of factors and their interactions on BP removal (%) in which the positive signs show enhance of response while the negative signs have the opposite effect.

$$R\%_{\text{butylparaben}} = 93.084 - 10.093X_1 - 3.340X_2 + 2.4167X_3 + 4.2700X_4 - 4.9075X_1X_2 - 1.3925X_1X_3 + 3.5525X_1X_4 + 0.89500X_2X_3 - 0.17500X_2X_4 - 0.44000X_3X_4 - 3.7119X_1^2 - 1.1059X_2^2 + 0.39410X_3^2 - 2.3559X_4^2 \quad (1)$$

Table 3. Analysis of Variance for the full quadratic model.

BP dye removal					
Source of variation	Df	Sum of square	Mean square	F-value	P-value
Model	14	4353.1	310.93	751.23	< 0.0001
X_1	1	1746.2	1746.2	4218.9	< 0.0001
X_2	1	267.73	267.73	646.86	< 0.0001
X_3	1	140.17	140.17	338.65	< 0.0001
X_4	1	437.59	437.59	1057.2	< 0.0001
X_1X_2	1	385.34	385.34	930.99	< 0.0001
X_1X_3	1	31.025	31.025	74.957	< 0.0001
X_1X_4	1	201.92	201.92	487.86	< 0.0001
X_2X_3	1	12.816	12.816	30.965	< 0.0001
X_2X_4	1	0.49	0.49	1.1839	0.29375
X_3X_4	1	3.0976	3.0976	7.4839	0.015321
X_3X_5	1	225.83	225.83	545.61	< 0.0001
X_1^2	1	33.962	33.962	82.053	< 0.0001
X_2^2	1	4.3128	4.3128	10.42	0.005631
X_3^2	1	154.12	154.12	372.37	< 0.0001
X_4^2	15	6.2085	0.4139	751.23	< 0.0001
Residual	9	5.1621	0.57357		
Lack of Fit	6	1.0464	0.1744	3.2889	0.080484
Pure Error	29	3251.3			

Modeling of ANN process

The network's function controls three functions weight (training), transfer, and net input. At epoch number 10, an mean square error (MSE) of 1/E83 (-8) for the ANN neural network model and MSE of 0.33 for the FL neuro-fuzzy model was spotted for the removal of BP dye. Because the network underwent a testing phase, training was halted, and weights have been frozen. The MSE vs. the number of epochs for the optimal ANN model is displayed in Figure 5. It should be noted that the training was halted after epoch numbers 10 and 50 experimental points for ultrasonic-assisted removal of BP dye. Also, as evident in Figures 5-8, in the MSE, all through the training process occurred. Apart from this, the errors in this removal process were very negligible, as was evident from the plot of the error histogram for the adsorption process shown in Figure 6. In the current article, during the net training process, the MSE had a minimum value of 5 neurons based upon error performance. An ANN model with four input layers namely initial BP dye, pH, adsorbent dosage, and ultrasonic time and premised on the output layers (deleting target compounds) was proved to be significantly reliable for predicting and reckoning the BP dye removal. In this model, MSE and the correlation coefficients (R^2) (Table 4) helped the training, testing, and validation for the removal of BP dye.

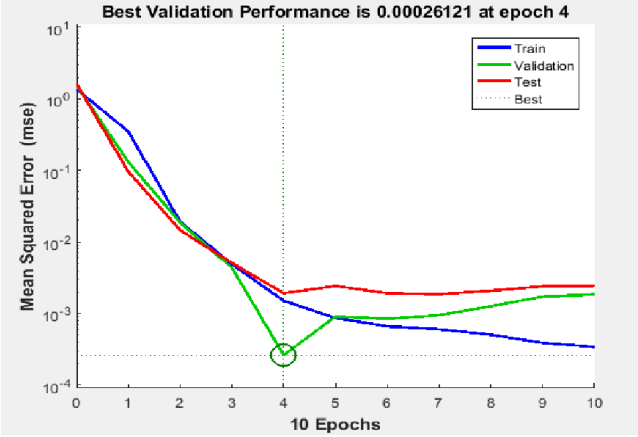

Figure 5. Gradual change of training, validation, and test errors as a function of the number of training epochs during ANN for the BP dye removal by ALLC AgNPs.

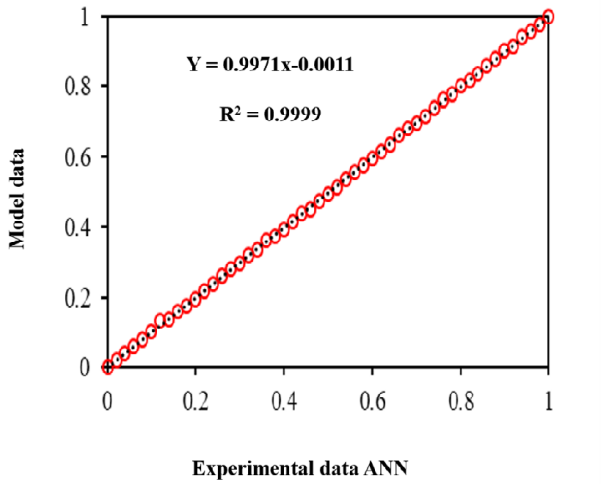

Figure 6. The Plot of the juxtaposition of factual (objective) data and predicted data of ANN neural network model and neuro-fuzzy model for the BP dye removal by ALLC AgNPs.

Table 4. Statistical comparison of two models of artificial neural networks.

SD	AARE	SSE	MSE	R^2	Model
0.148	0.028	9.E35(-7)	1.E83(-8)	0.9999	**ANN**
45.45	2.49	16.84	0.33	0.8331	**FL**

It can be seen that the sum of the squares of relative error, the mean of the sum of the squares of error, the mean of the absolute error, the standard deviation, and the correlation coefficient of the findings of all three models were juxtaposed. Also, the outcomes demonstrated the relative superiority of the neuro-fuzzy model and ANN neural network model. Moreover, the obtainment of the lowest determination errors for BP dye was possible within a very short time, which clearly showed the greater contribution of ALLC AgNPs in removing BP dye.

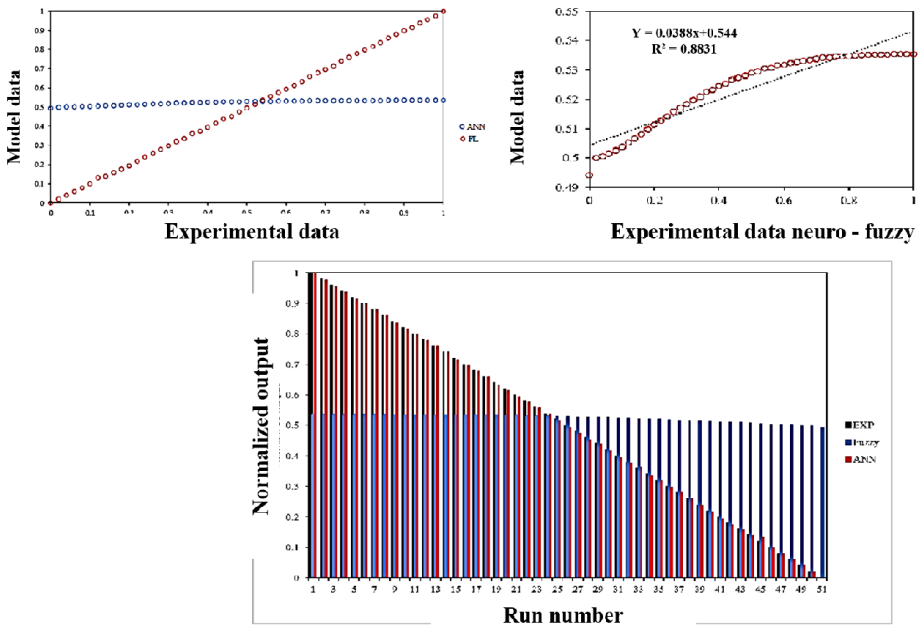

Figure 7. The Plot of the juxtaposition of histograms of factual and output data of ANN and FL models for the BP dye removal by ALLC AgNPs.

Response surface plots

RSM is indeed a 3-dimensional (3D) plot that can show the interactions of effective factors on the removal process simultaneously and also can follow their influences on removal percentage [31]. These plots are presented in Figure 9. As can be seen from these plots, they show the interaction of two factors. According to these plots, increasing adsorbent mass can increase the removal percentage. This is because increasing adsorbent mass can increase adsorption sites, functional groups, surface area, and adsorption capacity.

The ultrasonic time is another main factor that increasing can enhance the adsorption percentage. When ultrasonic irradiation is increased the possible interactions between BP dye molecules and adsorbent is increased which subsequently can raise the adsorption percentage. The pH of the solution is another main factor that can change the structure of adsorbent and dye molecules.

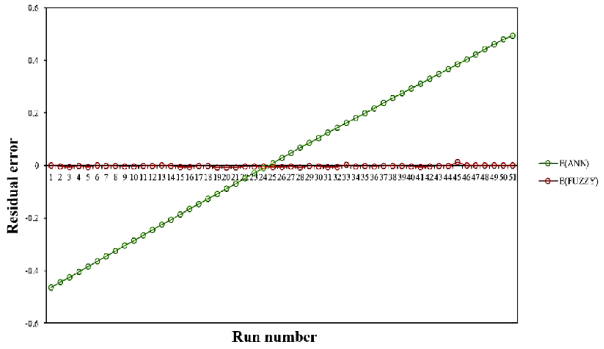

Figure 8. The Plot of juxtaposition of histograms of relative error of ANN and FL models for the BP dye removal by ALLC AgNPs.

At lower pH, due to the high concentration of hydrogen, the surface of the adsorbent can be protonated. In this manner, there are strong attraction forces between adsorbent and BP dye molecules. According to the structures of adsorbent and BP dye molecules, the adsorption mechanism can be attributed to the weak electrostatic interactions (physical adsorption) between BP dye molecules and AgNPs. Indeed, the adsorption mechanism is based on the interaction between the C=O, C-O, and O-H groups of BP with AgNPs. C=O, C-O and O-H groups of BP can act as electron donor groups and interact with AgNPs [32].

The maximum removal percentage was achieved under the following conditions: pH of 7.0, ultrasound time of 4.0 min, the adsorbent mass of 0.025 g, and initial BP dye concentration of 12 mg L^{-1}.

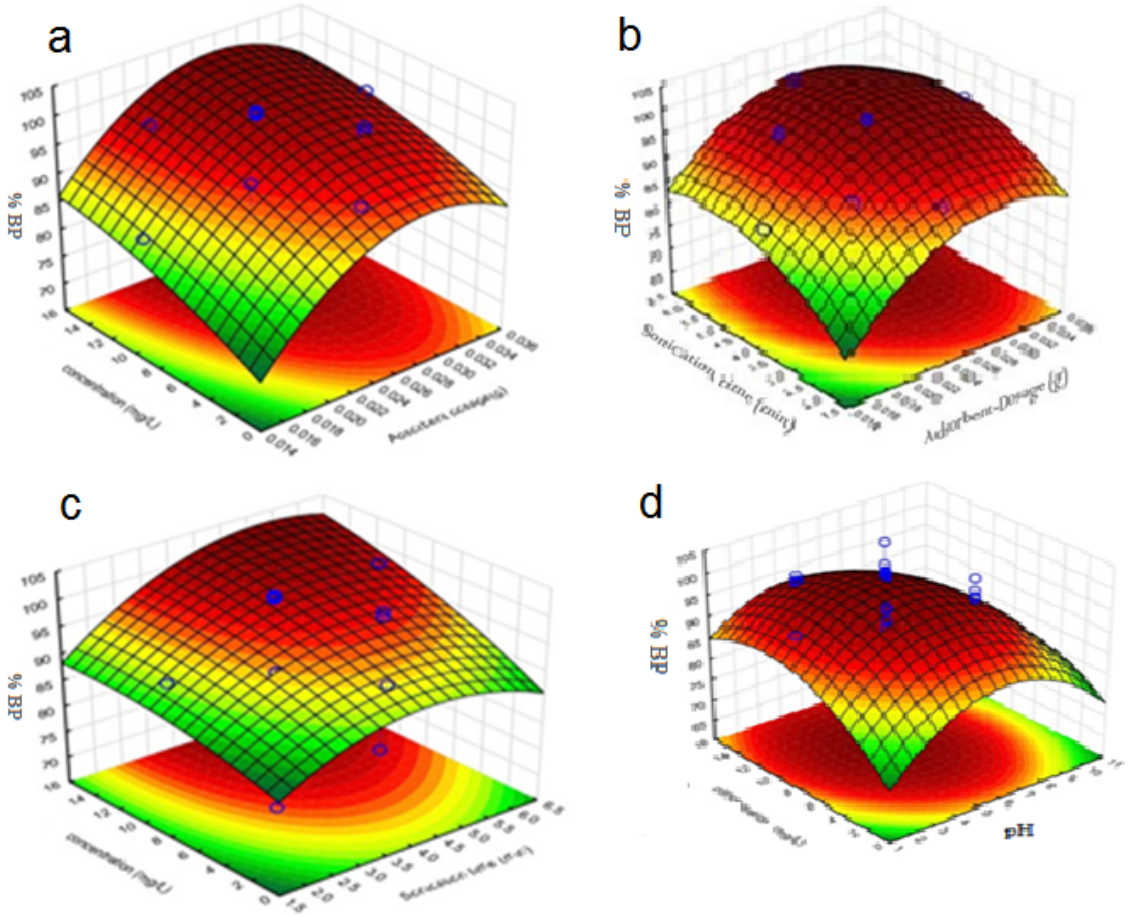

Figure 9. Response surfaces for the BP dye removal: (a) initial BP dye concentration–adsorbent dosage (b) time (min)–adsorbent dosage, (c) initial BP dye concentration– time (min), (d) initial BP dye concentration– pH.

Absorption isotherms

To investigate the adsorption mechanism and also to evaluate adsorbent behavior, different isotherm models were used. The assessed isotherms, their equation, and their explanation are presented in Table 5. According to the obtained results, the Langmuir adsorption isotherm model was selected as the best model [4]. It was due to its higher R^2 value (0.998) compared to other models. Langmuir model assumes the monolayer adsorption of dye molecules on the homogeneous surface of the adsorbent. It also proved that there are not any interactions between adsorbed molecules and the adsorption process on uniform surfaces. The principles of applied isotherm are explained in our last works.

The Temkin isotherm model was employed to assess the heat of the adsorption and the adsorbent–adsorbate interaction. B in the prior mentioned model refers to the Temkin constant, t stands for the heat of the adsorption (J/mol) and T (K), R(8.314 J/mol. K), and K (L/mg) represents the absolute temperature, the universal gas constant, and the equilibrium

binding constant respectively. The D-R model was considered appropriate for assessing the porosity, apparent free energy, and adsorption properties. To conclude, the Langmuir isotherm was nominated as the worthiest model to describe the butylparaben dye adsorption onto AALC AgNPs. The obtained maximum adsorption capacity from the Langmuir model was 100 mg g^{-1} which makes the fabricated adsorbent an ideal candidate for the removal of pollutants.

Table 5. Different isotherm models for BP dye adsorption onto ALLC Ag NPs.

Isotherms	Equation	parameters	Value of parameters For BP
Langmuir	$q_e=q_m bC_e/(1+bC_e)$	Q_m (mg g^{-1})	100
		K_a (L mg^{-1})	0.487
		R^2	0.998
Freundlich	$\ln q_e = \ln K_F + (1/n) \ln C_e$	1/n	0.55
		K_F (L mg^{-1})	4.09
		R^2	0.982
Tempkin	$q_e = B_1 \ln K_T + B_1 \ln C_e$	B_1	14.15
		K_T (L mg^{-1})	6.855
		R^2	0.978
Dubinin-Radushkevich (DR)	$\ln q_e = \ln Q_s - B\varepsilon^2$	Q_s (mg g^{-1})	39.64
		$B\times 10^{-7}$	-1
		E (kj mol^{-1})	2237
		R^2	0.963

Kinetic study

The kinetic reaction is another main factor in the removal process that can investigate the rate of adsorption [33]. To evaluate the rate of adsorption, various kinetic models were examined (Table 5). The principles of kinetic models are explained in the literature. According to the results, the pseudo-second-order model had a higher R^2 (0.9995) value that showed its higher suitability than other models.

Table 6. Kinetic parameters for the adsorption of BP dye onto ALLC Ag NPs.

Model	parameters	Value of parameters for BP
pseudo-First-order kinetic	k_1(min-1)	0.987
	qe (calc) (mg g-1)	17.92
	R^2	0.9498
pseudo-Second-order kinetic	k_2 (min-1)	0.154
	q_e(calc) (mg g^{-1})	56.15
	R^2	0.9995
Intraparticle diffusion	K_{diff} (mg g-1 min-1/2)	8.05
	C (mg g^{-1})	33.77
	R^2	0.9859
Elovich	β (g mg-1)	0.609
	α (mg g-1 min-1)	17.74
	R^2	0.9761

Recycling of the Adsorbent

Reusability of fabricated adsorbent is another main factor for its practical applications. The reusability of the proposed adsorbent was investigated in different cycles. Based on the obtained results (Figure 10), ALLC AgNPs were applicable for at least 6 cycles which makes them an excellent candidate for utilization as adsorbents.

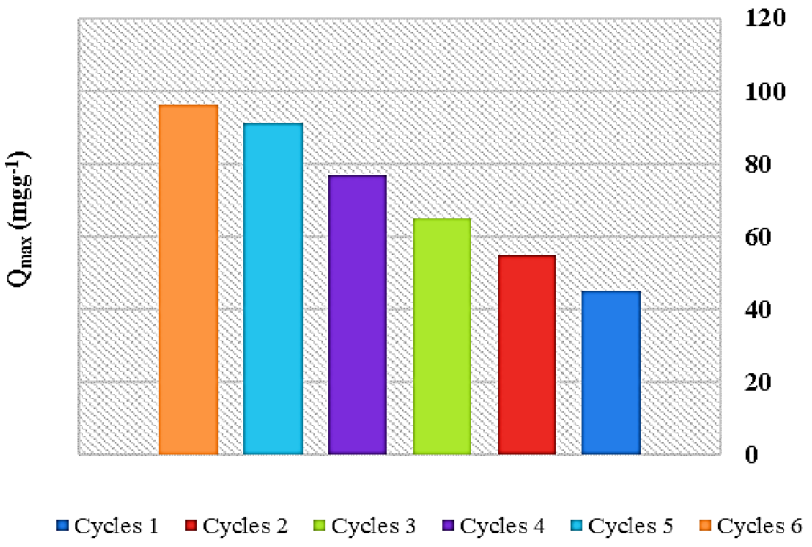

Figure 10. Desorption of BP dye onto ALLC AgNPs. [BP dye concentration= 12 mgL^{-1}; pH = 7.0; adsorbent dose = 0.025 g; time = 4.0 min].

Comparison of ALLLC AgNPs with other adsorbents

Table 7 represents the comparison of ALLC AgNPs with some other fabricated adsorbents. As shown in Table 7, constructed ALLC AgNPs in this work had higher or similar adsorption capacity compared to other adsorbents. The synthesized adsorbent in this study not only had high adsorption capacity but also had a simple, easy, cheap, available, and most importantly green and environmentally friendly synthesis approach. These exceptional features distinguish ALLC AgNPs from other adsorbents.

Table 7. Comparison of ALLLC AgNPs with other adsorbents.

Dyes	Adsorbent	Dosage sorbent (g)	Adsorption capacity	References
Rhodamine123 (R123) and Disulfine blue (DSB) dyes	Au–Fe_3O_4 NPs nanoparticles Loaded on Activated Carbon	0.025	71.46 mg g^{-1} and 76.38 mg g^{-1}	[34]
Disulfin Blue and Methyl dyes	Titanum Dioxide-NPs loaded onto Activated Carbon	0.25	70.3 mg g^{-1} and 48.48 mg g^{-1}	[35]
Orange 122 dye	Fe_3O_4 Magnetic Nanoparticles	1.4	51.546 mg g^{-1}	[36]
Reactive Red 120 dye	Albizia lebbeck Fruit (Pod)	0.05	1.68 mg g^{-1}	[37]
BP	Modified granular activated carbons prepared from African palm shell	-	0.74-1.38 mmol g^{-1}	[38]
BP	Activated carbon	-	7.519 mg g^{-1}	
BP	MOF-derived porous carbon coated lanthanum oxide	-	-	[39]
BP	Porous N-doped graphene based NiO composite	-	10.46 mg g^{-1}	[40]
BP	Micro- and mesoporous silica from coal fly ash	-	-	[41]
BP	Albizia Lebbeck Leaves-capped AgNPs	0.025	100 mg g^{-1}	This study

Conclusion

The aim of this work was the synthesis and characterization of Albizia Lebbeck Leaves-Capped AgNPs as an adsorbent to remove BP dye. The formation mechanism of ALLC AgNPs was also investigated. Central composite design-based-response surface methodology was used to assess the influence of effective parameters, their interactions, and achieving optimum conditions. The artificial neural network was also used to build up an empirical model. The excellent contribution of ALLC AgNPs in removing BP dye was confirmed when the lowest errors were never obtained. To evaluate the adsorption mechanism and also to investigate the kinetic reaction, different isotherm and kinetic models were examined. The isotherm and kinetic were followed by Langmuir and the pseudo-second-order model. The

exceptional properties of fabricated ALLC AgNPs like a simple, easy, cheap, available, green, and environmentally friendly fabricated method as well as its higher adsorption capacity and exclusive performance for removal of BP dye molecules, make it an appropriate adsorbent for the removal of pollutants and especially dyes molecules.

It assumed that the formation mechanism was based on redox reaction reactions in which the compound in extracted plants like polyphenols, and proteins act as ligands (electron donors) and interact with metal ions (Ag^{+}, Au^{3+}, Cu^{2+}, etc.) as electron acceptors and synthesis metal nanoparticles.

Acknowledgment

This work is supported partially by the Islamic Azad University, Branch of Omidiyeh, Iran, and theauthors would like to acknowledge and thank their support.

Data Availability

All data generated or analyzed during this study are included in this published article in form of figures and tables.

References

[1] O.S. Hassan, H.G. Salman, O.A. Hashem, A.M. Abass, A.M. Abass, *Syst. Rev. Pharm.,* 11, 369 (2020).

[2] E.A. López-Maldonado, M.T. Oropeza-Guzmán, *Chem. Eng. J.,* 423, 130210 (2021).

[3] A.R. Bagheri, N. Aramesh, J. Chen, W. Liu, W. Shen, S. Tang, H.K. Lee, *Anal. Chim. Acta.,* 339509 (2022).

[4] H. Gholami, M. Ghaedi, M. Arabi, A. Ostovan, A.R. Bagheri, H. Mohamedian, *ACS Omega.,* 4, 3839 (2019).

[5] N. Matwiejczuk, A. Galicka, M.M. Brzóska, *J. Appl. Toxicol.,* 40, 176 (2020).

[6] T. Yin, X. Zhu, I. Cheang, Y. Zhou, S. Liao, X. Lu, Y. Zhou, W. Yao, X. Li, H. Zhang, *Environ. Sci. Pollut. Res.,* 1 (2021).

[7] F. Peinado, O. Ocón-Hernández, L. Iribarne-Durán, F. Vela-Soria, A. Ubiña, C. Padilla, J. Mora, J. Cardona, J. León, M. Fernández, *Environ. Res.,* 196, 110342 (2021).

[8] M.J. Laws, A.M. Neff, E. Brehm, G.R. Warner, J.A. Flaws, *Adv. Pharmacol.,* 92, 151 (2021).

[9] J. Lin, T. Su, J. Chen, T. Xue, S. Yang, P. Guo, H. Lin, H. Wang, Y. Hong, Y. Su, *Chemosphere.,* 272, 129640 (2021).

[10] A.R. Bagheri, N. Aramesh, F. Sher, M. Bilal, *Chemosphere.,* 270, 129523 (2021).

[11] A.R. Bagheri, N. Aramesh, M. Bilal, J. Xiao, H.-W. Kim, B. Yan, *Biorg. Med. Chem.,* 51, 116493 (2021).

[12] A.R. Bagheri, N. Aramesh, M. Bilal, *Environ. Res.,* 194, 110654 (2021).

[13] I.M. Rashid, S.D. Salman, A.K. Mohammed, *Energy Ecol. Environ.,* 6, 1 (2021).

[14] S. Ibrahim, Z. Ahmad, M.Z. Manzoor, M. Mujahid, Z. Faheem, A. Adnan, *Sci. Rep.,* 11, 1 (2021)

[15] H.S.T.S.H. Abdullah, S.N.A.R.M. Asseri, W.N.K.W. Mohamad, S.-Y. Kan, A.A. Azmi, F.S.Y. Julius, P.W. Chia, *Environ. Pollut.,* 271, 116295 (2021).

[16] L. Niknam, F. Marahel, *J. Appl. Chem. Res.,* 18, 37 (2021).

[17] M. Rafique, I. Sadaf, M.B. Tahir, M.S. Rafique, G. Nabi, T. Iqbal, K. Sughra, *Mater. Sci. Eng. C.,* 99, 1313 (2019).

[18] F. Félix-Domínguez, R. Carrillo-Torres, A. Lucero-Acuña, R. Sánchez-Zeferino, M. Álvarez-Ramos, *Mater. Res. Express.,* 6, 125060 (2019).

[19] S. Kiamarzi, M. Abrishamkar, A. Maleki, F. Marahel, *Int. J. Environ. Anal. Chem.,* 1 (2021).

[20] C.R. Sahoo, S. Maharana, C.P. Mandhata, A.K. Bishoyi, S.K. Paidesetty, R.N. Padhy, *J. Biol. Sci.,* 27, 1580 (2020).

[21] G.L. Vanti, M. Kurjogi, K. Basavesha, N.L. Teradal, S. Masaphy, V.B. Nargund, *J. Biotechnol.,* 309, 20 (2020).

[22] A. Kumar, A.A. Kumar, A.P. Nayak, P. Mishra, M. Panigrahy, P.K. Sahoo, K.C. Panigrahi, *J. Biosci.,* 44, 6 (2019).

[23] P. Xu, Y. Wang, C. Cen, M. Zheng, Z. Wu, M. Zhou, J. Fei, Z. Teng, *J. Taiwan Inst. Chem. Eng.,* 112, 162 (2020).

[24] M.R. Piani, M. Abrishamkar, B.M. Goodajdar, M. Hossieni, *Desalin. Water Treat,* 213, 288 (2021).

[25] H. Gholami, M. Arabi, M. Ghaedi, A. Ostovan, A.R. Bagheri, *J. Chromatogr. A.,* 1594, 13 (2019).

[26] A.R. Bagheri, M. Ghaedi, A. Asfaram, R. Jannesar, A. Goudarzi, *Ultrason. Sonochem.,* 35, 112 (2017).

[27] L.G. Cardoso, D.S. Madeira, T.E. Ricomini, R.A. Miranda, T.G. Brito, E.J. Paiva, *Int. J. Adv. Manuf. Syst.,* 1, 42 (2021).

[28] S.S. Yang, X.L. Yu, M.Q. Ding, L. He, G.L. Cao, L. Zhao, Y. Tao, J.W. Pang, S.W. Bai, J. Ding, *Water Res.,* 189, 116576 (2021).

[29] F. Maghami, M. Abrishamkar, B.M. Goodajdar, M. Hossieni, *Desalin. Water Treat.,* 228, 376 (2021).

[30] A.R. Bagheri, M. Ghaedi, *Arab. J. Chem.,* 13, 5218 (2020).

[31] M.S. Surya, G. Prasanthi, S. Gugulothu, *Silicon,* 1 (2021).

[32] K. Dastafkan, M. Khajeh, M. Bohlooli, M. Ghaffari-Moghaddam, N. Sheibani.*Talanta,* 144, 1377 (2015).

[33] A.R. Bagheri, M. Arabi, M. Ghaedi, A. Ostovan, X. Wang, J. Li, L. Chen, *Talanta,* 195, 390, (2019).

[34] S. Bagheri, H. Aghaei, M. Ghaedi, A. Asfaram, M. Monajemi, A.A. Bazrafshan, *Ultrason. Sonochem.,* 41, 279 (2018).

[35] M.R. Parvizi, N. Karachi, *Orient. J. Chem.,* 33, 2559 (2017).

[36] S.H. Ahmadi, P. Davari, A. Manbohi, *Iran. J. Chem. Eng.,* 35, 63 (2016).

[37] G. Haghdoost, *J. Phys. Chem.,* 4, 141 (2019).

[38] A.R. Moreno-Marenco, L. Giraldo, J.C. Moreno-Piraján, *J. Environ. Chem. Eng.,* 8,103969 (2020).

[39] C. Chen, L. Xu, J.B. Huo, K. Gupta, M.L. Fu, *Chem. Eng. J.,* 391, 123552 (2020).

[40] D.Z. Husein, *Desalin. Water. Treat.,*166, 211 (2019).

[41] F.F. de Oliveira, K.O. Moura, L.S. Costa, C.B. Vidal, A.R. Loiola, R.F. do Nascimento, *ACS Omega,* 5, 3346 (2020).